

# Phosphatidic Acid Improves Reprogramming to Pluripotency by Reducing Apoptosis

Yuan Jiang,<sup>1,2,\*</sup> Mingxia Du,<sup>1,3,\*</sup> Menghua Wu,<sup>1,2</sup> Yanbing Zhu,<sup>1,2</sup> Xing Zhao,<sup>1,2</sup>  
Xu Cao,<sup>1,2</sup> Xin Li,<sup>1,2</sup> Peipei Long,<sup>1,2</sup> Wei Li,<sup>1,2</sup> and Baoyang Hu<sup>1,2</sup>

Generation of induced pluripotent stem cells (iPSCs) requires a considerable amount of lipids, such as phosphatidic acid (PA), to meet the needs of subsequent rapid cell division and proliferation. However, it is unclear whether PA, a biosynthetic precursor of lipids, affects reprogramming. By using lentiviral expression of the Yamanaka factors in mouse embryonic fibroblasts for reprogramming, we identified that PA is beneficial for the generation of iPS colonies. Inhibiting the generation of cellular PA dramatically decreased the number of iPSCs. Consistently, 400  $\mu$ M PA improved iPSC generation by more than 4- to 5-fold. iPSCs generated in the presence of PA (PA-iPS) expressed pluripotent markers such as *Oct4* and *Nanog*, differentiated into cells of the three germ layers in vitro, and contributed to chimeric mice when injected into blastocysts. The improved efficiency was primarily due to reduction of apoptosis as sufficient PA increased the accumulation of cardiolipin in the inner membrane of the mitochondria, which reduced the release of cytochrome *c* and, in turn, suppressed apoptosis by inhibiting caspase-7. The relatively higher amount of Bcl-2 in PA treatment also inhibited apoptosis. In addition, an accompanied sequential change from epithelial-to-mesenchymal transition (EMT) at the initial phase of reprogramming to mesenchymal-to-epithelial transition (MET) was also detected. Our microarray data, which also supported our results, indicated the presence of significant membrane enrichment genes, thus suggesting that PA may function through membrane-anchored proteins. We thus identified a novel type of culture supplement that improves the efficiency of reprogramming and could be valuable for the generation of high-quality iPS cells.

## Introduction

INDUCED PLURIPOTENT STEM CELLS (iPSCs) generated through exogenous expression of defined factors such as Oct4, Sox2, Klf4, and *c-Myc* (OSKM) in somatic cells offer tremendous opportunities for stem cell research and applications [1–4]. However, several issues, arising from the generation of iPSCs, have hindered their practical application in basic research, drug screening, and medical therapy. In addition to the enhanced tumorigenicity of iPSCs that are generated using oncogenes (eg, *c-Myc*) [5], the efficiency of iPSC generation, which is usually lower than 1%, has long been the focus of investigations. The quality of iPSCs, which is also related to their heterogeneity [1,6], has also attracted much attention because only ~1 in 10 colonies can be sufficiently reprogrammed to be chimera competent [7].

Several critical aspects during reprogramming such as culture conditions and supplements [8] in addition to their stoichiometry [9] may affect the efficiency of reprogramming and quality of the iPSCs.

Higher efficiency of iPSC generation is usually achieved through removal of reprogramming barriers, inhibition of apoptosis, and improvement of the survival of the reprogrammed cells. The natural compound ascorbic acid (vitamin C, Vc) serves as a repressor of p53/p21 and an epigenetic regulator to boost iPSC generation [10,11]. Growth factors such as fibroblast growth factor 2 (FGF2) reduce levels of extracellular matrix proteins that hamper cell reprogramming and, thus, play a positive role in iPSC generation [12–14]. These strategies to improve the efficiency of iPSC generation have been evaluated quantitatively but not qualitatively, and it is also not clear whether the improvement of iPSC generation efficiency affects the quality of reprogramming.

Phosphatidic acid (PA), among other lipids, is emerging as an important mediator in diverse cellular functions across multiple species. PA is a biosynthetic precursor of acylglycerol lipids and is produced by enzymes such as phospholipase D (PLD) and diacylglycerol (DAG) kinase (DGK) [15–18]. Under physiological conditions, PLD catalyzes the hydrolysis of phospholipids, mainly phosphatidylcholine

<sup>1</sup>The State Key Laboratory of Reproductive Biology, Institute of Zoology, Chinese Academy of Sciences, Beijing, China.

<sup>2</sup>University of Chinese Academy of Sciences, Beijing, China.

<sup>3</sup>School of Life Sciences, Anhui University, Hefei, China.

\*These authors contributed equally to this work.

(PC), resulting in the formation of PA [19]. PA alone can function as a cellular messenger [20], or it can be transformed by PA phosphohydrolase into diacylglycerol, which is essential for activation of protein kinase C (PKC) [21,22].

In other complicated cellular activities such as vesicular trafficking, secretion and endocytosis, oxidative bursting, cytoskeletal dynamics, and cell differentiation, PA plays important roles through membrane tethering to regulate enzymatic activity or affect membrane fluidity. PA also mediates intramitochondrial cardiolipin (CL) synthesis to improve the apoptotic resistance through TRIAP1/PRELI complexes [23]. The cellular functions of PA are spatiotemporally specific and regulated by activation of distinct PA-generating enzymes at different times and in different subcellular compartments [16,24]. It is not clear, however, whether the presence of PA affects the reprogramming somatic cells to iPS cells.

## Materials and Methods

### Cell culture

Mouse embryonic fibroblasts (MEFs) were isolated from E13.5 embryos heterozygous for the *Oct4::GFP* transgenic allele, as previously described [25]. Feeder cells were harvested from the CF1 mouse strain (SLRC). Other mouse strains used in this research were obtained from Vital River Company. J1-129 mouse embryonic stem cells (mESCs) were used as a positive control.

HEK293T cells and MEFs were cultured in Dulbecco's modified Eagle's medium (DMEM), 10% fetal bovine serum (FBS), 1% GlutaMAX, and 1% nonessential amino acids (all from Life Technologies). mESCs and iPSCs were maintained on Gu60-radiated MEFs in ESC culture medium containing KnockOut DMEM, 15% knockout serum replacement or 15% FBS, 1% GlutaMAX, 1% nonessential amino acids, 1% penicillin–streptomycin, 1% sodium pyruvate, 0.1 mM 2-mercaptoethanol (all from Gibco), and 1,000 U/mL leukemia inhibitory factor (LIF; Millipore). iPSCs were generated in N2B27 medium consisting of 48% DMEM/F12, 48% neurobasal medium, 0.5% N<sub>2</sub>, 1% B27 (all from Gibco), insulin (Roche), bovine serum albumin (Sigma), and 1,000 U/mL LIF. MEFs, ESCs, and iPSCs were passaged with 0.25% trypsin (Gibco), and 293T cells were passaged with 0.05% trypsin (Gibco).

### Generation of iPS cells

Preparation of lentiviruses and the procedure for iPS cell derivation were conducted as previously described [26–28]. Briefly, medium containing the lentiviruses TetO-FUW-OSKM (*Oct4*, *Sox2*, *Klf4*, and *c-Myc*) and FUW-M2rtTA (20321 and 20342; Addgene) was harvested after 48 and 72 h of transfection in HEK293T cells. MEFs (10<sup>5</sup>) cultured for 24 h on a gelatin-coated dish in DMEM and 10% FBS (Gibco) were transduced for 16–18 h with the collected virus. After 1–2 days, MEFs were passaged onto the feeder MEFs at 25,000 cells/well (six-well plate) in N2B27 medium supplemented with inhibitors of ERK (PD0325901, 1 μM; Stemgent) and GSK3β (CHIR99021, 3 μM; Stemgent) and 2 μg/mL doxycycline to induce expression of the four reprogramming factors. PA was added at different culture stages as indicated. Inhibitors of PLD1/2 (VU0155056), PLD1 (PLD1i,

VU0359595), and PLD2 (PLD2i, VU0285655-1) were from Avanti Polar Lipids. The DGK inhibitor (DGKi) R59022 was from Calbiochem. Positive colonies were mechanically picked up on day 14 and cultured on feeder cells.

### Differentiation of iPSCs in vitro

For embryoid body (EB) formation, cells were harvested by trypsinization and plated at a concentration of 5 × 10<sup>6</sup> cells/10-cm dish on nonadherent culture dishes in ESC medium without LIF. The cells were gently blown when changing the medium every 2 days. After 3 days in suspension, EBs were plated on gelatin-coated dishes and incubated for another 3 days. The cells were stained with anti-α-smooth muscle actin monoclonal antibody (N1584; Dako), anti-α-fetoprotein polyclonal antibody (N1501; Dako), or anti-βIII tubulin monoclonal antibody (CBL412; Abcam) with Hoechst 33342 (Sigma).

### Immunofluorescence staining and AP staining

Cells fixed with 4% paraformaldehyde in phosphate-buffered saline (PBS) at room temperature for 30 min were permeabilized in PBST (PBS with 0.3% Triton X-100; 3 × 5 min) and incubated with blocking buffer [3% (v/v) normal donkey serum in PBST], each for 30 min. Slides were incubated with primary antibodies diluted in antibody buffer [1% (v/v) normal donkey serum in PBST] at 4°C overnight. The following primary antibodies were used: rabbit anti-Oct4 (ab19857; Abcam), rabbit anti-Nanog (a300-397A; Bethyl), and mouse anti-stage-specific embryonic antigen1 (anti-SSEA1) (MAB4301; Millipore). Slides were washed in PBST, thrice each for 5 min. Alexa Fluor 594 donkey anti-rabbit (A21207; Invitrogen) and Alexa Fluor 594 donkey anti-mouse (A21203; Invitrogen) antibodies were added and incubated in the dark at room temperature for 1 h. Slides were washed in PBS thrice each for 5 min, and the DNA was labeled by Hoechst 33342. Stained cells were mounted and observed on a LSM 780 META microscope (Zeiss).

Alkaline phosphatase staining was performed with the BCIP/NBT Alkaline Phosphatase Color Development Kit (C3206; Beyotime) according to the manufacturer's instructions.

### Quantitative real-time reverse transcription polymerase chain reaction

Total RNA was extracted manually with TRIzol Reagent (Invitrogen). cDNA was synthesized using 1 μg of RNA, M-MLV reverse transcriptase (Promega), and RNasein RNase inhibitor (Promega). Quantitative reverse transcription polymerase chain reaction (PCR) was conducted with SYBR Premix Ex Taq (Promega) and the primers listed in Supplementary Table S1 (Supplementary materials are available online at [www.liebertpub.com/scd](http://www.liebertpub.com/scd)). Expression values were normalized to those of *Gapdh* and relative to those of control samples. Error bars represent the mean ± SD of two or three independent experiments.

### Western blot analysis

Whole-cell extracts were obtained with RIPA lysis buffer (89900; Thermo) supplemented with protease inhibitor (Roche Applied Science), then quantified using a BCA protein assay kit (23225; Thermo). After electrophoresis, proteins were

transferred to nitrocellulose membranes. Primary antibodies against E-cadherin (#3195; Cell Signaling Technology), Nanog (A300-397A; Bethyl), Sox2 (AB5603; Millipore), Caspase-7 (ab181579; Abcam), Zeb1 (ABN285; Millipore), Bax (2772; Cell Signaling Technology), Bcl-2 (2876; Cell Signaling Technology), and  $\beta$ -Actin (60008-1-Ig; Proteintech) were used. Horseradish peroxidase-conjugated secondary antibodies against rabbit or goat IgG were also used (ZSGB-BIO).

#### *Teratoma formation and histological analysis*

In total,  $1 \times 10^6$  PA-iPS cells were injected subcutaneously into each flank of recipient NOD/SCID mice. Tumors were surgically dissected 4–5 weeks after the injection, weighed, fixed in PBS containing 4% formaldehyde, and embedded in paraffin. Sections were stained with hematoxylin and eosin (H&E).

#### *Chimera generation*

Chimera generation was performed using protocols reported previously [1]. PA-iPS cells and control cells propagated from six individual iPSC colonies were microinjected into the host embryos using a flat-tip microinjection pipette. Each blastocyst received 10–12 iPS cells. Two hours after injection, blastocysts were transferred into the uterus of day 2.5 recipient ICR female mice (20 blastocysts per female). When the chimeric mice reached adulthood, they were mated with ICR mice to test germ-line transmission.

#### *Apoptosis analysis*

Apoptosis analysis was performed using the Annexin V-PE/7-AAD Apoptosis Detection Kit (559763; BD Pharmingen) according to the manufacturer's instructions. TUNEL assay was executed with the Alexa Fluor 647 TUNEL Detection Kit (40308; YEASEN).

#### *Microarray analysis*

Total RNA was extracted from MEFs treated with or untreated PA for 7 days after induction using TRIzol reagent (Invitrogen). Samples were prepared in three biological replicates. Total RNA was quantified by NanoDrop ND-2000 spectroscopy (Thermo Scientific), and RNA integrity was assessed on an Agilent Bioanalyzer 2100 (Agilent Technologies). The sample labeling, microarray hybridization, and washing were performed according to the manufacturers' standard protocols. After washing, the arrays were scanned with an Agilent Scanner G2505C (Agilent Technologies).

Feature Extraction software (version 10.7.1.1; Agilent Technologies) was used to analyze array images to obtain raw data. GeneSpring was used to finish the basic analysis of the raw data. Differentially expressed genes were then identified through fold change and  $P$  values calculated by  $t$  test. The threshold set for up- and downregulation of genes was  $\geq 2.0$ -fold and  $P \leq 0.05$ . Subsequently, gene ontology (GO) and KEGG analyses were used to determine the roles of these differentially expressed mRNAs. Finally, hierarchical clustering was performed to display the expression patterns between samples.

## Results

### *PA improves reprogramming efficiency*

To identify the effect of PA on reprogramming, we designed the scheme as shown in Supplementary Fig. S1. We used tet-on expression of the Oct4, Sox2, Klf4, and c-Myc transcription factors in MEFs that were derived from *Oct4*-GFP (OG2) transgenic mice [25]. Cells were treated with different concentrations of exogenous PA (100–800  $\mu$ M) during reprogramming, and the control groups were treated with the same amount of PBS.

At the early stage of reprogramming, no significant morphological differences were observed between the PA-treated cells and the control group (data not shown). On day 10–14 of reprogramming, the number of AP-stained colonies in both reached a plateau. After 12 days of induction, substantially more AP-positive colonies were observed in cells treated with PA than in the control group (Fig. 1A). In particular, cells treated with 400  $\mu$ M PA exhibited the highest proportion of GFP-positive cells as determined by flow cytometry (PA 37.30% vs. 8.77% control) (Fig. 1B), as well as the highest number of *Oct4*-GFP-positive and AP-positive colonies (4- to 5-fold higher in the PA group vs. the controls) (Fig. 1B–D). All the coincident results suggest that 400  $\mu$ M PA promotes reprogramming significantly.

Because PA is primarily produced by PLD and DGK, we used inhibitors of PLD and DGK (PLDi, 0.75  $\mu$ M; DGKi, 10  $\mu$ M, respectively) to block the production of endogenous PA to determine whether cellular PA really affects cell reprogramming. In the presence of either PLDi or DGKi alone, no obvious decrease in iPSC colony number was observed (Fig. 1E), indicating that repression of only one route of PA generation did not significantly inhibit PA production. When both PLDi and DGKi were used together, few or no iPSC colonies appeared, indicating that PA production was completely blocked and that endogenous PA is critical for successful reprogramming (Fig. 1F).

### *PA promotes iPSCs generation at the early to middle stage of reprogramming*

To elucidate the dynamic roles of PA in promoting somatic cell reprogramming, we added exogenous PA in the culture medium at different stages of reprogramming (days 1–3, 3–6, 6–9, 3–9, and 3–14) and counted the number of GFP- and AP-positive colonies. All PA-treated groups, regardless of the stage at which PA was added, showed a dramatic increase in iPSC generation versus the control group (Fig. 1G–H). Among the various stages when PA was added, PA supplementation at day 3–9 produced the number of iPSC colonies,  $\sim 3$ -fold more than in the control group (Fig. 1G–H). These results indicated that treatment of somatic cells with PA during the early to middle phase of reprogramming is the most effective for improving reprogramming efficiency.

### *iPSCs generated in the presence of PA (PA-iPSCs) are pluripotent*

To investigate whether the iPSC cell lines derived from *Oct4*-GFP MEFs in the presence of PA (PA-iPSCs) were pluripotent, we examined the expression of several classical pluripotent markers by PCR, western blot, and immunostaining.

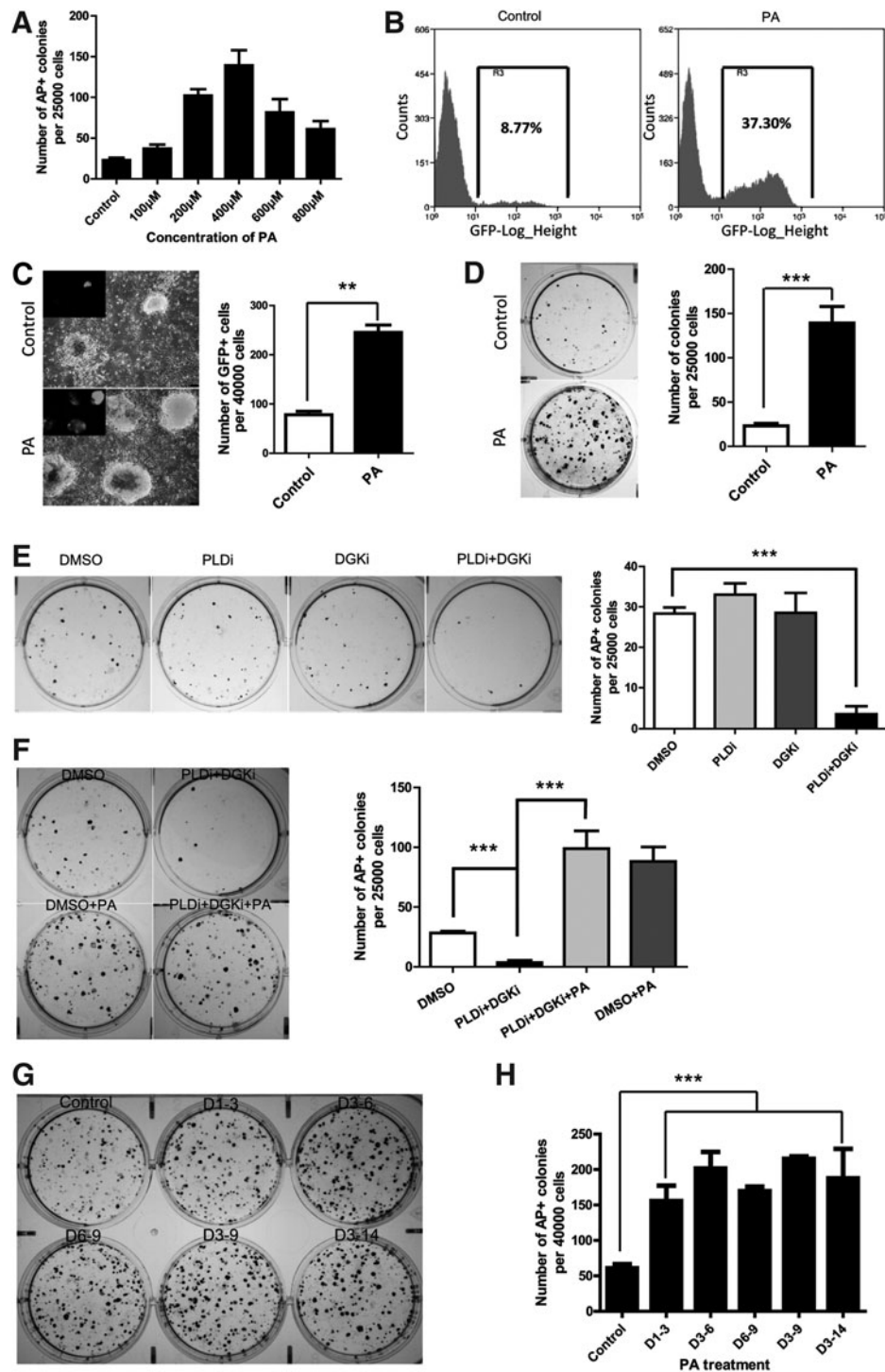


**FIG. 1.** PA enhances reprogramming of mouse fibroblasts. **(A)** Counts of AP<sup>+</sup> colonies at different PA concentrations indicated that 400 μM PA yielded the highest number of AP<sup>+</sup> colonies. **(B)** Representative graphs of FACS showing the proportion of GFP-positive cells (representing iPS cells that are Oct4 positive) in the control and PA group (400 μM) at day 14 of reprogramming. **(C) Left:** Representative phase contrast and fluorescence images of OSKM-transduced MEFs untreated or treated with PA. **Right:** Statistical analysis of GFP-positive colonies. **(D) Left:** Representative images of AP staining of reprogrammed cells with or without 400 μM PA. **Right:** Statistical analysis of AP<sup>+</sup> colonies. **(E) Left:** Representative images of AP staining with or without the PA inhibitor. No obvious differences were detected between groups treated with PLDi (0.75 μM) or DGK inhibitor (DGKi, 10 μM). In the presence of both inhibitors, few or no iPS colonies appeared. **Right:** Statistical analysis of AP<sup>+</sup> colonies in different groups. **(F) Left:** Representative AP staining showing exogenous PA rescued iPS generation when endogenous PA was inhibited. **Right:** Statistical analysis of AP<sup>+</sup> colonies in the left panel. **(G)** Representative images of AP staining on day 14 showing the number of iPS colonies in the presence of PA over the course of iPS generation. **(H)** Statistical analysis of AP<sup>+</sup> colonies in **(G)**. Data shown are representative of at least three independent experiments. Mean value ± SD is shown. \*\**P* < 0.01, \*\*\**P* < 0.001. iPSCs, induced pluripotent stem cells; MEF, mouse embryonic fibroblast; PA, phosphatidic acid; PLD, phospholipase D; PLDi, PLD inhibitor.

The PA-iPS colonies expressed a bright GFP signal from the *Oct4* locus and could be long-term passaged as AP positive. Comparable expression of *Oct4*, *Esrrb*, and *Lin28a* mRNA was observed in PA-iPSCs and the mESC line (Fig. 2A and Supplementary Fig. S2). In addition, other ES marker genes, including *Nanog*, *E-cadherin*, *Fbx15*, *Dppa2*, and *Gdf3*, were highly expressed in the PA-iPS cells compared with control cells (Fig. 2B and Supplementary Fig. S2), thus indicating that

these PA-iPS cells were of better quality. Pluripotent transcription factors such as Oct4 and Nanog together with pluripotent surface marker stage-specific embryonic antigen 1 (SSEA1) were also detected in the PA-iPS cell lines by immunofluorescence staining (Fig. 2C).

The iPS cell lines generated in the presence of PA formed EBs in vitro when harvested by trypsinization and transferred to bacterial culture dishes in ES medium without LIF.

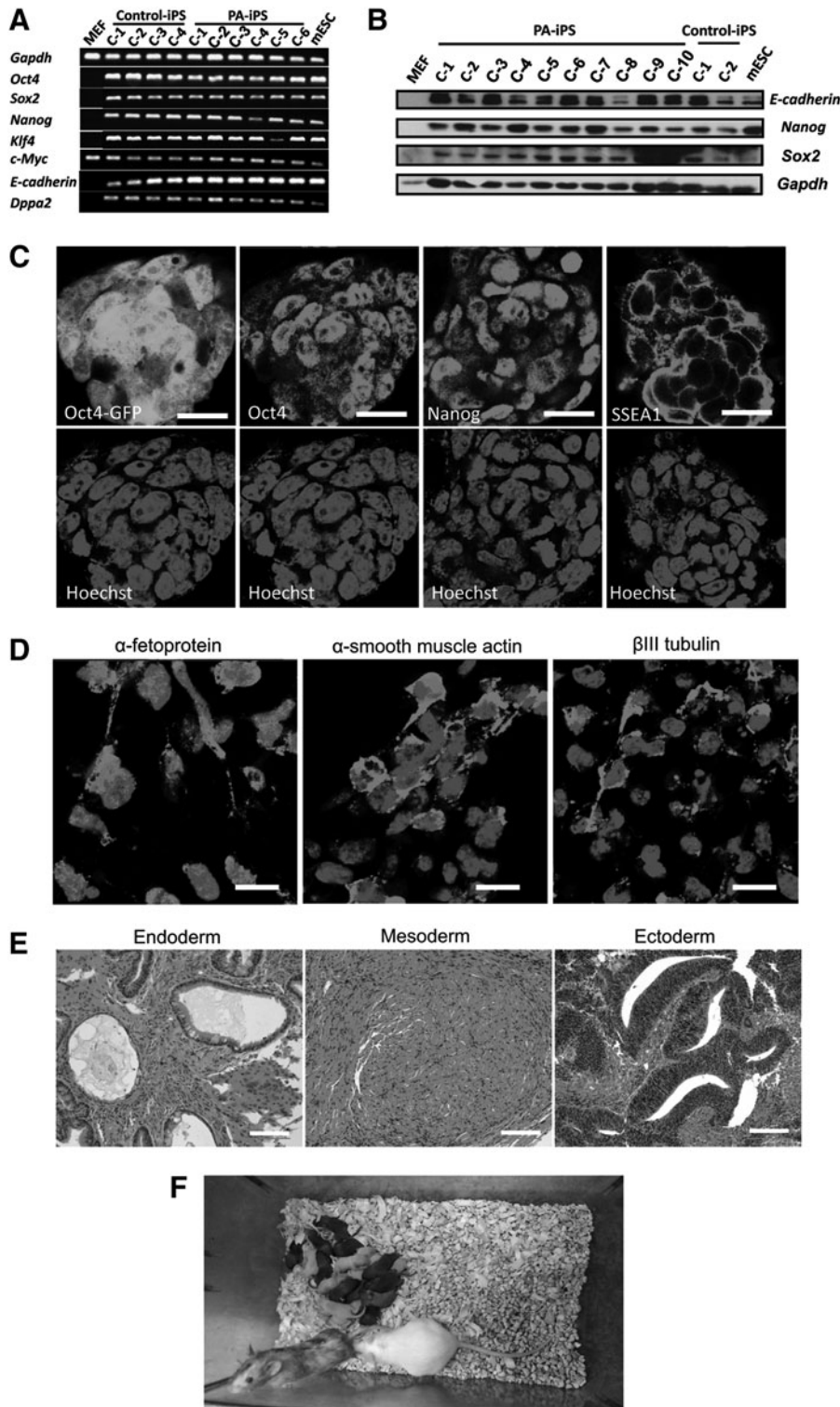


**FIG. 2.** Pluripotency of iPS lines generated in the presence of PA. **(A)** Comparable mRNA levels of pluripotency markers in four control iPSC lines (C-1 to C-4), six PA-iPSC lines (C-1 to C-6), and control mESC lines. **(B)** Western blotting to show pluripotency markers in 10 PA-iPSC lines, 2 control iPSC lines, and mESC lines. *Gapdh* is the loading control. **(C)** Images showing endogenous Oct4 (*Oct4*-GFP) and immunostaining of Oct4, Nanog, and SSEA-1 in representative PA-iPSC colonies. Scale bar: 20  $\mu$ m. **(D)** Immunostaining showing markers of the three germ layers when PA-iPSCs were differentiated in vitro. Scale bar: 10  $\mu$ m. **(E)** Images of hematoxylin and eosin (H&E)-stained samples representing all three germ layers from teratomas derived from the PA-iPS cells. Scale bar: 100  $\mu$ m. **(F)** Chimeric mice generated from PA-iPS cells showed germ-line transmission. mESCs, mouse embryonic stem cells.

These EBs adhered to the bottom of the dish 3 days later, and the cells in the EBs stained positive for  $\alpha$ -fetoprotein (endoderm marker),  $\alpha$ -smooth muscle actin (mesoderm marker), and  $\beta$ III tubulin (ectoderm marker) (Fig. 2D). These results demonstrate the pluripotent nature of the PA-iPS cells.

The PA-iPS cell lines, when subcutaneously injected into NOD/SCID mice, contributed to the formation of well-differentiated teratomas containing tissues representing all three germ layers (representative images in Fig. 2E). When injected into blastocysts, the PA-iPS cells effectively contributed to chimeric mice; moreover, chimeric mice generated from PA-iPS cells showed germ-line transmission ability when they were mated with ICR mice that had reached adulthood (Fig. 2F). All chimeric mice generated from independent clones grew to old age without any obvious evidence of tumorigenicity.

Furthermore, we compared differentiation capabilities, teratoma and chimera formation, and found no significant difference between control and PA-iPS cells, although we got a higher level expression for pluripotent genes (Supplementary Fig. S2), and a greater degree of the contribution in coat color of individual chimeras with PA-iPS cells (data not shown).

#### *PA treatment reduces apoptosis during PA-iPSC generation*

To systematically address how PA improves reprogramming efficiency, we first evaluated proliferation during reprogramming by measuring the ratio of the total cell number to the colony number. We did not observe any significant difference between control and PA-treated reprogramming at any of the time points evaluated (data not shown). However, we found that in the control groups without PA treatment, the shape of iPSC colonies was irregular and some cells in these colonies disappeared at the late stage of reprogramming, especially in the case of colonies on days 10 and 12 in the control group (Fig. 3A). In the groups with PA treatment, the colonies were much larger and there were very few irregular colonies (Fig. 3A). These results indicate that during the process of iPSC generation, the cells endure severe stress and a portion of them undergo apoptosis. Furthermore, we observed more chromatin condensation in morphology in the control group than in PA-treated cells on day 8 through DNA-specific dyeing with Hoechst 33342 (Supplementary Fig. S3A, B).

We thus employed flow cytometry to analyze the cell apoptosis during reprogramming. Before the apoptosis analysis, almost all of the inactivated feeder cells were removed from the digested cells using a differential adhesion method with gelatin. By analyzing the portion of cells that were 7-AAD negative and positive for PE Annexin V, a marker of cells undergoing apoptosis, we found that in the early stage (days 4–6) of reprogramming, there were no distinct differences in the rate of apoptosis. Nevertheless, from day 7 to day 12 of reprogramming, a growing population of apoptotic cells was present in the control group (from 14.8% to 60.8%) in comparison to the PA-treated group, in which the portion of cells undergoing apoptosis was much smaller (from 7.02% to 14.0%) (Fig. 3B, C). We also statistically analyzed the cells that are both PE Annexin V and 7-AAD positive in late apoptosis or already dead

(Fig. 3C, right panel). However, the differences are not significant as in cell apoptosis for PE Annexin V positive only (Fig. 3C, left panel), despite both positive cell ratios reduced in PA treatment. Moreover, we also carried out an apoptosis assay using the removed feeder cells, and the results indicated that most of the feeder cells died due to weak adhesion and mechanical damage for long cultivation; only a few feeder cells underwent apoptosis, and there was no significant difference between the control and PA group (Supplementary Fig. S3C, D). So the reduced number of cells that are both PE Annexin V and 7-AAD positive may be caused by decreased cell apoptosis rather than cell death in PA treatments.

We also performed TUNEL assay during reprogramming (Supplementary Fig. S3E, F). The results also support that PA treatment reduced apoptosis during reprogramming. However, different from the Annexin V detection, higher numbers of cell apoptosis were detected at day 4 of reprogramming, and less dUTP labeled cells were captured at the late stage of reprogramming. A reasonable explanation maybe that the TUNEL method is mainly used to detect the early fracture of genomic DNA in cell apoptosis, and in late a mass of genome degradation, resulting in the TUNEL label decreased. In addition, large DNA fragment fracture cannot be captured by the TUNEL method.

In addition, we also detected the expression of caspase-3 and caspase-7, the executives of caspase, and observed that the expression of activated caspase-7 in the PA group was lower than in the control group (Fig. 3D). Thus, we conclude that the improved efficiency of iPSC generation in the presence of PA is a result of inhibition of cell apoptosis during the reprogramming.

#### *EMT-MET transition during PA reprogramming*

During the PA-iPS cell generation, we detected a sequential change from pro-epithelial-to-mesenchymal transition (EMT) to pro-mesenchymal-to-epithelial transition (MET), which could potentially improve reprogramming [29]. In comparison to the control group, the expression of epithelial genes such as *E-cadherin*, *Ep-Cam*, and *Cldn3* was repressed during the first 4 days of OSKM induction (Fig. 4A), accompanied by concurrent upregulation of mesenchymal or EMT-related genes such as *Zeb1*, *Zeb2*, and *N-cadherin*. After this initial period, *Zeb1* and *N-cadherin* were sharply repressed followed by gradual repression of *Zeb2*. PA treatment induced a continuous increase in *Ep-Cam* and *E-Cadherin* expression until reprogramming was nearly complete at day 12 (Fig. 4A). Besides the quantitative PCR (qPCR) analysis, the expression of mesenchymal and epithelial genes at protein level was analyzed through western blot. The results also showed an early EMT process before MET transition, as indicated by the upregulation of *Zeb1* followed by the increased expression of E-cadherin (Fig. 4B).

#### *Alteration of gene expression profile in the presence of PA during reprogramming*

To further investigate the molecular mechanisms by which PA promotes reprogramming, we performed a microarray analysis and compared global gene expression profiles during reprogramming in the presence or absence of PA at day 7 of reprogramming. Hierarchical clustering

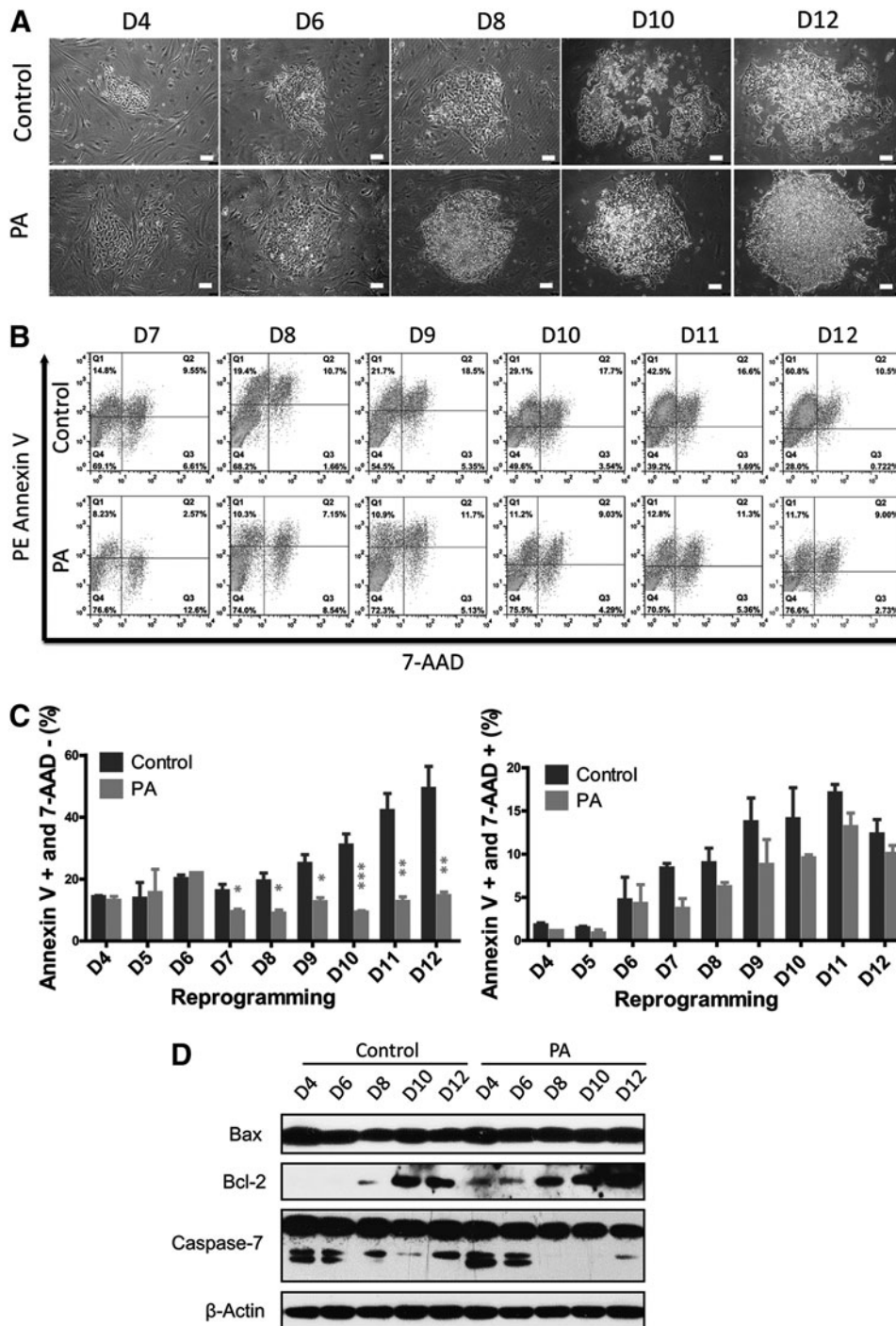


**FIG. 3.** PA reduces apoptosis during reprogramming. **(A)** Bright-field images showing the morphological differences between control and PA groups during reprogramming. Scale bar: 100  $\mu$ m. **(B)** Apoptosis in reprogrammed cells during iPSC generation. **(C)** Quantitative analysis of data illustrated in **(B)**. *Left:* PE Annexin V-positive and 7-AAD-negative staining shows the percentage of cells in early apoptosis. *Right:* Both PE Annexin V positive and 7-AAD show the percentage of cells in late apoptosis or already dead. **(D)** Western blotting to show differences in expression of apoptosis-related proteins between control and PA treatment during reprogramming.  $\beta$ -Actin is the loading control. D, day of reprogramming.

showed that the gene expression was distinct between the two groups (Fig. 5A). Among the 318 differentially expressed genes, 119 were upregulated and 199 were downregulated in the PA group.

GO data showed that the vast majority (69.3%) of the products of the differentially expressed genes belonged to the membrane, with 35.9% genes residing on the plasma membrane according to cellular component analyses (Fig. 5B). In terms of molecular function, 19.4% of the products of the genes play roles as the way of protein binding and the others mainly exhibit peptidase inhibitor activity, ion channel activity, and transcription activator activity, with each ac-

counted for 8.7% of the genes (Fig. 5B). Pathway analysis of these of the products of the differentially expressed genes using the KEGG database indicated that 26.2% of them were enriched for the neuroactive ligand–receptor interaction pathway, 19% belonged to the calcium-signaling pathway, and 16.7% of them exhibited cytokine–cytokine receptor interactions (Fig. 5C).

We also further quantified the mRNA level of differentially expressed genes between two groups. The cell apoptosis-related genes, such as *Bcl2ald* and *Aifm2*, the apoptosis-inducing factor, and mitochondrion-associated 2, were downregulated in PA treatment compared to control

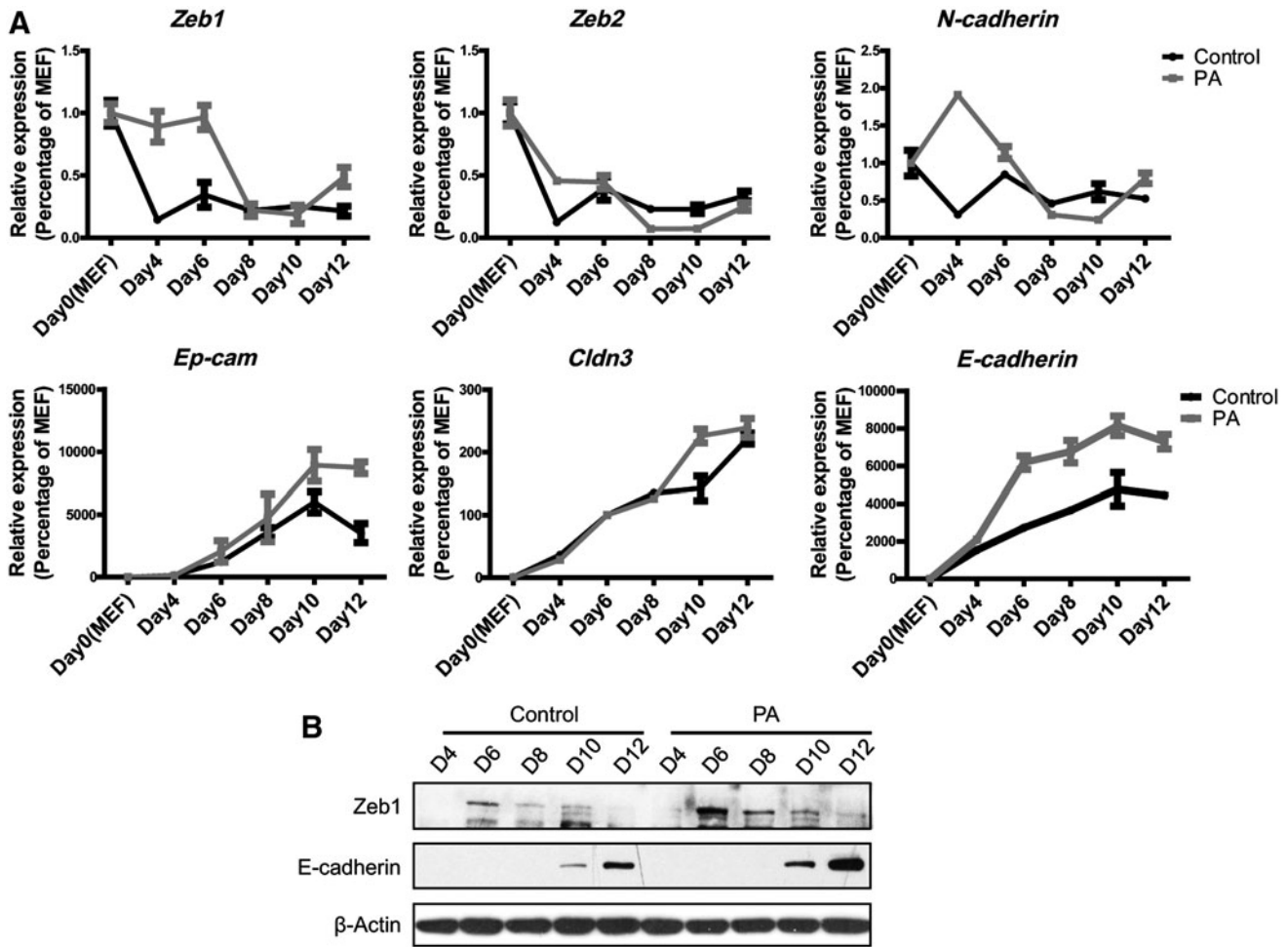


**FIG. 4.** EMT-MET transition during PA reprogramming. (A) Expression of EMT- and MET-related genes as determined by quantitative PCR during reprogramming. Data are presented as mean  $\pm$  SD of triplicate wells from representative experiments. (B) Western blotting for ZEB1 and E-cadherin in lysates from reprogrammed cells of untreated or treated PA.  $\beta$ -Actin is the loading control. EMT, epithelial-to-mesenchymal transition; MET, mesenchymal-to-epithelial transition; PCR, polymerase chain reaction.

cells (Fig. 5D), and that is consistent with our results from the apoptosis analysis. Furthermore, genes related to cell membrane components and function (binding or interaction with channel-related proteins) were also identified. For example, *S100a3* (S100 calcium binding protein A3), *Eras* (ES cell-expressed Ras), and *Crisp3* (cysteine-rich secretory protein 3) were upregulated, while the expression level of *Ms4a7* (membrane-spanning 4A gene family), *Cib3* (calcium and integrin binding family member 3), and *Igfbp3* (insulin-like growth factor binding protein 3) was downregulated (Fig. 5D). However, the detail mechanisms need further research. In conclusion, the microarray data showed that the genes affected by PA were largely related to cell membrane components and that their products may function through binding or interaction with channel-related proteins.

Based on the results, we thus put forward a hypothetical model for the function of PA in cell apoptosis (Fig. 6). It needs a lot of lipids, such as PA, during somatic reprogramming to allow rapid cell division and proliferation. The mitochondrial signature lipid CL directly binds to cytochrome c (Cyt *c*), and whic is retained within the cristae and

regulates multiple steps of apoptosis [30]. The lack of CL accumulation in the cristae induces the release of cytochrome c (Cyt *c*) from the mitochondria to the spanning channel and renders the cells vulnerable to apoptosis upon intrinsic and extrinsic stimulation (Fig. 6A). PA, as a precursor of CL synthesis, increases the accumulation of CL in the inner membrane, which reduces the release of Cyt *c* and, in turn, decreases cell apoptosis through inhibiting the expression of caspase-7, the executor of apoptosis. In addition, the relatively higher amount of Bcl-2 than Bax was detected also to promote the inhibition of cell apoptosis by formation of heterodimer Bcl-2/Bax and Bcl-2 homodimer (Fig. 6B).

## Discussion

In this study, we identified a type of lipid that can be used as a novel culture supplement to improve the efficiency of reprogramming without compromising the quality of the resulting iPSCs. The increased reprogramming efficiency may be caused by decreased cell apoptosis, accompanied by sequential EMT-MET transition of PA-iPSCs. This is the



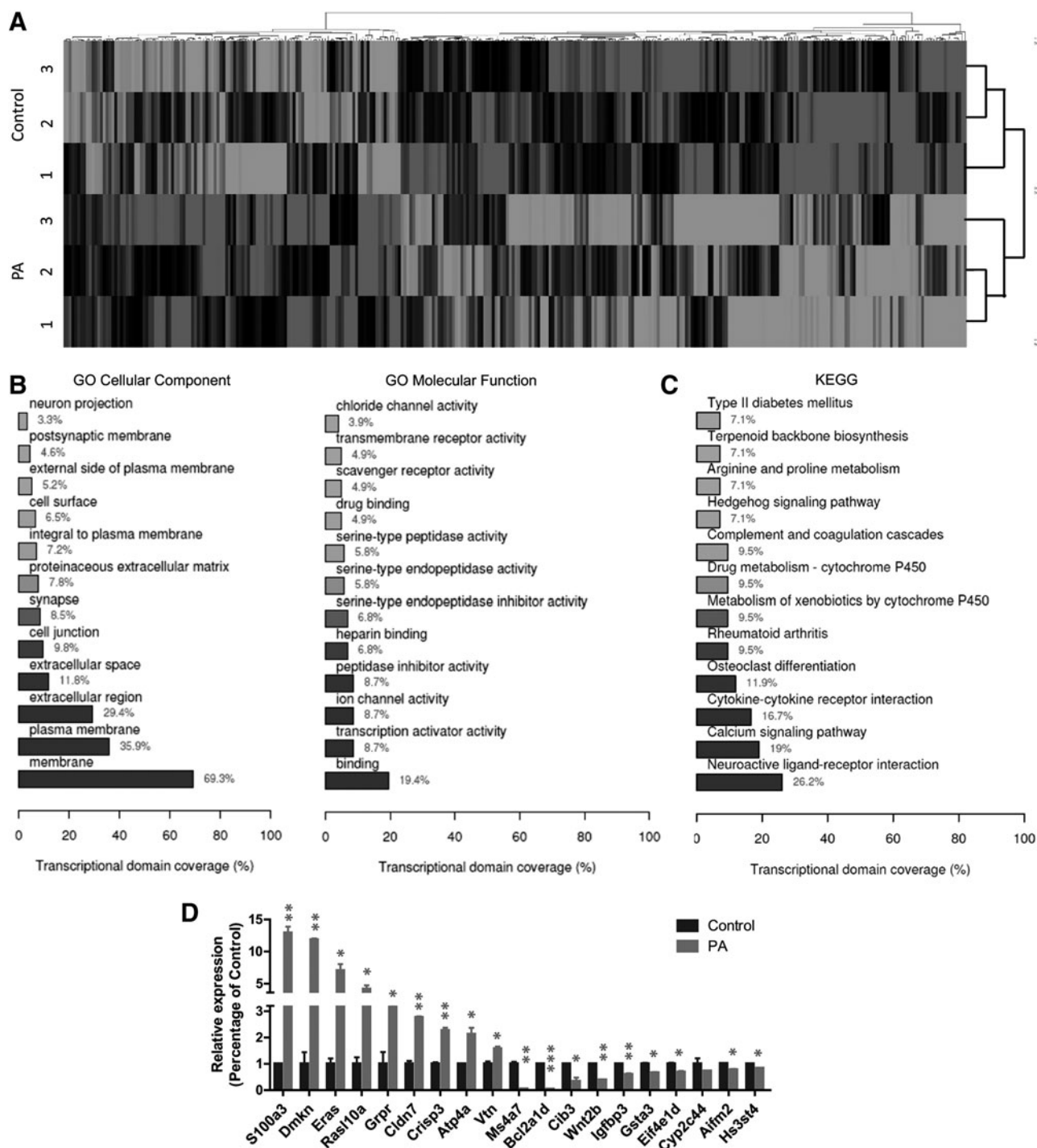


**FIG. 5.** Gene expression profile of cells during reprogramming. **(A)** Hierarchical clustering based on differential screening of 319 genes derived from reprogrammed cells (at day 7) untreated and treated with PA. **(B)** GO analysis of differentially expressed genes in terms of cellular components and molecular function. **(C)** KEGG signaling pathway analysis of genes influenced by PA during reprogramming. **(D)** Relative expression of representative genes corresponds to quantitative PCR analysis of **(A)** during reprogramming. Data are presented as mean  $\pm$  SD of triplicate wells from representative experiments. \* $P < 0.05$ , \*\* $P < 0.01$ , \*\*\* $P < 0.001$ .

first report that PA, the simplest cell lipid, can improve the efficacy of iPSC cell generation at the early to middle stages of reprogramming.

Since Takahashi and Yamanaka first reported the iPSC technology [3], many efforts have made to develop safer and more effective methods for reprogramming of somatic cells.

As reprogramming is cell cycle dependent, the initial focus of improving the reprogramming was the inhibition of tentative barriers of cell cycling such as p53 signaling [31–34]. Subsequently, vitamin C, a common nutrient vital to human health, was identified as an enhancer of reprogramming of somatic cells to pluripotent stem cells, as it improves the

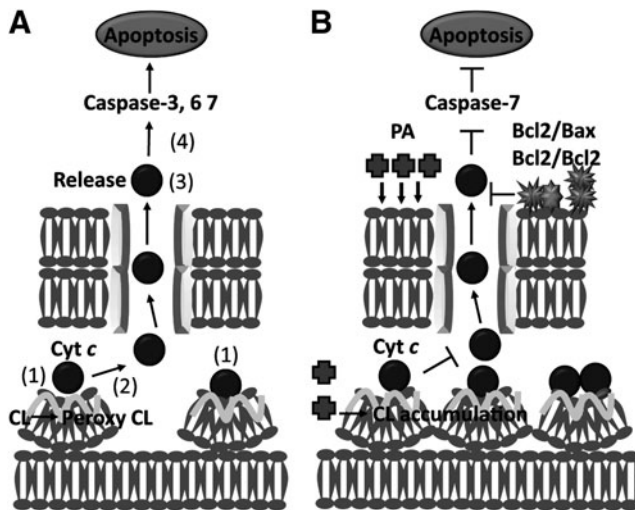


**FIG. 6.** A hypothesized model for the function of PA in cell apoptosis during reprogramming. **(A)** (1) Cytochrome *c* (Cyt *c*) binds to CL (the mitochondrial signature lipid CL) in the inner mitochondrial membrane. (2) The accumulation of CL decreased because of a requirement of large quantities of lipids and, especially, PA (the precursor of lipid synthesis) for cell division and proliferation during somatic reprogramming. Cyt *c* is released upon oxidation of CL. (3) Cyt *c* is released from mitochondria through a spanning channel. (4) Cells are rendered susceptible to apoptosis upon intrinsic and extrinsic stimulation. **(B)** Exogenous PA, when added during reprogramming as a precursor of CL synthesis, increases accumulation of CL in the inner mitochondrial membrane, which reduces the release of Cyt *c*, and suppresses cell apoptosis through inhibition of Caspase-7 expression. Formation of the Bcl-2/Bax heterodimer and Bcl-2 homodimer, because of the relatively high amount of Bcl-2 compared to that of Bax, also inhibits apoptosis during this process. CL, cardiolipin.

quality of the cells and generates tetraploid complementation-competent iPSCs even when a suboptimal factor stoichiometry is used to induce pluripotency [10,11]. Other small molecules that are known to be effective in regulating epigenetic status or signaling pathways, such as valproic acid (VPA, an HDAC inhibitor), AZA (a DNMT inhibitor), butyrate (an HDAC inhibitor), CHIR99021 (a GSK3 $\beta$  inhibitor), and PD0325901 (a MEK/ERK inhibitor) [7,35–38], have been intensively investigated and found to affect reprogramming.

However, the effects of lipids, which are endogenous cell components, have largely not attracted attention. Because PA has emerged as a new class of lipid mediator involved in diverse cellular functions [39–42], we chose it as a candidate for improving reprogramming. The effects of PA appear to be robust and versatile; it increased the number of iPSCs but did not affect their quality, at least according to the currently available assays. The increase in number of iPSCs was primarily due to the ability of PA to reduce cell apoptosis.

We have found a decreased percentage of cells that are PE Annexin V positive in early apoptosis, and detected a relatively higher expression of Bcl-2 than Bax, and the decreased expression of *Aifm2* and caspase-7 in PA-treated reprogramming based on our biochemical and molecular analysis. These results could give us a reasonable illustra-

tion for PA prompt reprogramming by inhibiting apoptosis. Combined with microarray analysis, we summarize the PA function as a hypothesis model (Fig. 6). Intramitochondrial transport of PA promotes the synthesis of CL, which retains Cyt *c* at the mitochondrial inner membrane, resulting in decreased cell apoptosis through inhibiting caspase-7. The relatively higher amount of Bcl-2 in PA treatment also inhibited the apoptosis process by oligomerization of BCL2 family members in the outer membrane. Reportedly, this process also triggers caspase-8 activation and formation of tBid during mitochondrial amplification of extrinsic apoptotic signals [31,43]. During cell reprogramming, deficiency of PA may impair CL accumulation, facilitating the release of Cyt *c* and rendering cells vulnerable to apoptosis; PA supplementation should alleviate this effect.

As we all know, an MET is essential to reprogramming; however, in the presence of PA, we also observed a significant sequential change from EMT to MET during reprogramming. This early or temporary EMT at the initial phase of reprogramming is helpful for somatic cells reprogramming. As MEFs are normally isolated at embryonic day 13.5 and are heterogeneous, PA, through an early EMT process, might have synchronized the MEFs closer to a mesenchymal ground state, from which MET can be initiated by the reprogramming factors toward pluripotency as reported previously [44]. A temporary EMT at the initial phase of reprogramming and the final MET are important for successful reprogramming, as reported in previous investigations [44,45].

Overall, we identified PA as an important molecule for cell reprogramming, and supplementation with PA at the early to middle phase significantly improved the efficiency of somatic reprogramming. Although the mechanisms of how PA enhances reprogramming require further investigation, harvesting of increased numbers of iPSCs simply by adding a simple lipid to the culture recipe is valuable both for studying the mechanisms of cell fate determination and for production of large amounts of iPSCs for translational purposes.

## Acknowledgments

This work was supported by grants from the Ministry of Science and Technology of China (2014CB964604, 2012CB966302) and the “Strategic Priority Research Program” of the Chinese Academy of Sciences (no. XDA01040109). The authors thank Dr. Tongbiao Zhao of the Institute of Zoology and CAS for providing materials and technical support.

## Author Disclosure Statement

The authors declare that they have no conflicts of interest. All of the authors have approved the article and agree with submission to your esteemed journal. All of the animal experimental procedures complied with the instructions for the Care and Use of Animals in Research published by the Institute of Zoology of the Chinese Academy of Sciences.

## References

1. Buganim Y, S Markoulaki, N van Wietmarschen, H Hoke, T Wu, K Ganz, B Akhtar-Zaidi, Y He, BJ Abraham, et al.

- (2014). The developmental potential of iPSCs is greatly influenced by reprogramming factor selection. *Cell Stem Cell* 15:295–309.
2. Takahashi K, K Tanabe, M Ohnuki, M Narita, T Ichisaka, K Tomoda and S Yamanaka. (2007). Induction of pluripotent stem cells from adult human fibroblasts by defined factors. *Cell* 131:861–872.
  3. Takahashi K and S Yamanaka. (2006). Induction of pluripotent stem cells from mouse embryonic and adult fibroblast cultures by defined factors. *Cell* 126:663–676.
  4. Yu JY, MA Vodyanik, K Smuga-Otto, J Antosiewicz-Bourget, JL Frane, S Tian, J Nie, GA Jonsdottir, V Ruotti, et al. (2007). Induced pluripotent stem cell lines derived from human somatic cells. *Science* 318:1917–1920.
  5. Ben-David U and N Benvenisty. (2011). The tumorigenicity of human embryonic and induced pluripotent stem cells. *Nat Rev Cancer* 11:268–277.
  6. Kim K, A Doi, B Wen, K Ng, R Zhao, P Cahan, J Kim, MJ Aryee, H Ji, et al. (2010). Epigenetic memory in induced pluripotent stem cells. *Nature* 467:285–290.
  7. Silva J, O Barrandon, J Nichols, J Kawaguchi, TW Theunissen and A Smith. (2008). Promotion of reprogramming to ground state pluripotency by signal inhibition. *PLoS Biol* 6:e253.
  8. Chen JK, J Liu, Y Chen, JQ Yang, J Chen, H Liu, XJ Zhao, KL Mo, H Song, et al. (2011). Rational optimization of reprogramming culture conditions for the generation of induced pluripotent stem cells with ultra-high efficiency and fast kinetics. *Cell Res* 21:884–894.
  9. Carey BW, S Markoulaki, JH Hanna, DA Faddah, Y Buganim, J Kim, K Ganz, EJ Steine, JP Cassady, et al. (2011). Reprogramming factor stoichiometry influences the epigenetic state and biological properties of induced pluripotent stem cells. *Cell Stem Cell* 9:588–598.
  10. Esteban MA and DQ Pei. (2012). Vitamin C improves the quality of somatic cell reprogramming. *Nat Genet* 44:366–367.
  11. Stadtfeld M, E Apostolou, F Ferrari, J Choi, RM Walsh, TP Chen, SSK Ooi, SY Kim, TH Bestor, et al. (2012). Ascorbic acid prevents loss of Dlk1-Dio3 imprinting and facilitates generation of all-iPS cell mice from terminally differentiated B cells. *Nat Genet* 44:398–405.
  12. Han DW, B Greber, GM Wu, N Tapia, MJ Arauzo-Bravo, K Ko, C Bernemann, M Stehling and HR Scholer. (2011). Direct reprogramming of fibroblasts into epiblast stem cells. *Nat Cell Biol* 13:66–71.
  13. Jiao J, YJ Dang, YY Yang, R Gao, Y Zhang, ZH Kou, XF Sun and SR Gao. (2013). Promoting reprogramming by FGF2 reveals that the extracellular matrix is a barrier for reprogramming fibroblasts to pluripotency. *Stem Cells* 31:729–740.
  14. Chen JK, J Liu, QK Han, DJ Qin, JY Xu, Y Chen, JQ Yang, H Song, DS Yang, et al. (2010). Towards an optimized culture medium for the generation of mouse induced pluripotent stem cells. *J Biol Chem* 285:31066–31072.
  15. Peng X and MA Frohman. (2012). Mammalian phospholipase D physiological and pathological roles. *Acta Physiol (Oxf)* 204:219–226.
  16. Selvy PE, RR Lavieri, CW Lindsley and HA Brown. (2011). Phospholipase D: enzymology, functionality, and chemical modulation. *Chem Rev* 111:6064–6119.
  17. Shulga YV, MK Topham and RM Epan. (2011). Regulation and functions of diacylglycerol kinases. *Chem Rev* 111:6186–6208.
  18. Zhang Y and G Du. (2009). Phosphatidic acid signaling regulation of Ras superfamily of small guanosine triphosphatases. *Biochim Biophys Acta* 1791:850–855.
  19. Liscovitch M, M Czarny, G Fiucci and X Tang. (2000). Phospholipase D: molecular and cell biology of a novel gene family. *Biochem J* 345 Pt 3:401–415.
  20. Exton JH. (1997). Phospholipase D: enzymology, mechanisms of regulation, and function. *Physiol Rev* 77:303–320.
  21. Gomez-Cambronero J and P Keire. (1998). Phospholipase D: a novel major player in signal transduction. *Cell Signal* 10:387–397.
  22. Nishizuka Y. (1995). Protein kinase C and lipid signaling for sustained cellular responses. *FASEB J* 9:484–496.
  23. Potting C, T Tatsuta, T Konig, M Haag, T Wai, MJ Aaltonen and T Langer. (2013). TRIAP1/PRELI complexes prevent apoptosis by mediating intramitochondrial transport of phosphatidic acid. *Cell Metab* 18:287–295.
  24. Wang X, SP Devaiah, W Zhang and R Welti. (2006). Signaling functions of phosphatidic acid. *Prog Lipid Res* 45:250–278.
  25. Boiani M, S Eckardt, HR Scholer and KJ McLaughlin. (2002). Oct4 distribution and level in mouse clones: consequences for pluripotency. *Genes Dev* 16:1209–1219.
  26. Brambrink T, R Foreman, GG Welstead, CJ Lengner, M Wernig, H Suh and R Jaenisch. (2008). Sequential expression of pluripotency markers during direct reprogramming of mouse somatic cells. *Cell Stem Cell* 2:151–159.
  27. Kang L, J Wang, Y Zhang, Z Kou and S Gao. (2009). iPSCs can support full-term development of tetraploid blastocyst-complemented embryos. *Cell Stem Cell* 5:135–138.
  28. Stadtfeld M, N Maherali, DT Breault and K Hochedlinger. (2008). Defining molecular cornerstones during fibroblast to iPS cell reprogramming in mouse. *Cell Stem Cell* 2:230–240.
  29. Liu X, H Sun, J Qi, L Wang, S He, J Liu, C Feng, C Chen, W Li, et al. (2013). Sequential introduction of reprogramming factors reveals a time-sensitive requirement for individual factors and a sequential EMT-MET mechanism for optimal reprogramming. *Nat Cell Biol* 15:829–838.
  30. Osman C, DR Voelker and T Langer. (2011). Making heads or tails of phospholipids in mitochondria. *J Cell Biol* 192:7–16.
  31. Kawamura T, J Suzuki, YV Wang, S Menendez, LB Morera, A Raya, GM Wahl and JC Izpisua Belmonte. (2009). Linking the p53 tumour suppressor pathway to somatic cell reprogramming. *Nature* 460:140–144.
  32. Li H, M Collado, A Villasante, K Strati, S Ortega, M Canamero, MA Blasco and M Serrano. (2009). The Ink4/Arf locus is a barrier for iPS cell reprogramming. *Nature* 460:1136–1139.
  33. Marion RM, K Strati, H Li, M Murga, R Blanco, S Ortega, O Fernandez-Capetillo, M Serrano and MA Blasco. (2009). A p53-mediated DNA damage response limits reprogramming to ensure iPS cell genomic integrity. *Nature* 460:1149–1153.
  34. Utikal J, JM Polo, M Stadtfeld, N Maherali, W Kulalert, RM Walsh, A Khalil, JG Rheinwald and K Hochedlinger. (2009). Immortalization eliminates a roadblock during cellular reprogramming into iPS cells. *Nature* 460:1145–1148.
  35. Huangfu DW, R Maehr, WJ Guo, A Eijkelenboom, M Snitow, AE Chen and DA Melton. (2008). Induction of pluripotent stem cells by defined factors is greatly improved by small-molecule compounds. *Nat Biotechnol* 26:795–797.

36. Esteban MA, T Wang, B Qin, J Yang, D Qin, J Cai, W Li, Z Weng, J Chen, et al. (2010). Vitamin C enhances the generation of mouse and human induced pluripotent stem cells. *Cell Stem Cell* 6:71–79.
37. Mali P, BK Chou, J Yen, ZH Ye, JZ Zou, S Dowey, RA Brodsky, JE Ohm, WN Yu, et al. (2010). Butyrate greatly enhances derivation of human induced pluripotent stem cells by promoting epigenetic remodeling and the expression of pluripotency-associated genes. *Stem Cells* 28:713–720.
38. Mikkelsen TS, J Hanna, XL Zhang, MC Ku, M Wernig, P Schorderet, BE Bernstein, R Jaenisch, ES Lander and A Meissner. (2008). Dissecting direct reprogramming through integrative genomic analysis. *Nature* 454:49–55.
39. Exton JH. (2002). Phospholipase D-structure, regulation and function. *Rev Physiol Biochem Pharmacol* 144:1–94.
40. Foster DA and L Xu. (2003). Phospholipase D in cell proliferation and cancer. *Mol Cancer Res* 1:789–800.
41. Jenkins GM and MA Frohman. (2005). Phospholipase D: a lipid centric review. *Cell Mol Life Sci* 62:2305–2316.
42. McDermott M, MJ Wakelam and AJ Morris. (2004). Phospholipase D. *Biochem Cell Biol* 82:225–253.
43. Gonzalez F, ZT Schug, RH Houtkooper, ED MacKenzie, DG Brooks, RJA Wanders, PX Petit, FM Vaz and E Gottlieb. (2008). Cardiolipin provides an essential activating platform for caspase-8 on mitochondria. *J Cell Biol* 183:681–696.
44. Li RH, JL Liang, S Ni, T Zhou, XB Qing, HP Li, WZ He, JK Chen, F Li, et al. (2010). A mesenchymal-to-epithelial transition initiates and is required for the nuclear reprogramming of mouse fibroblasts. *Cell Stem Cell* 7:51–63.
45. Samavarchi-Tehrani P, A Golipour, L David, HK Sung, TA Beyer, A Datti, K Woltjen, A Nagy and JL Wrana. (2010). Functional genomics reveals a BMP-driven mesenchymal-to-epithelial transition in the initiation of somatic cell reprogramming. *Cell Stem Cell* 7:64–77.

Address correspondence to:

*Prof. Baoyang Hu*

*The State Key Laboratory of Reproductive Biology*

*Institute of Zoology*

*Chinese Academy of Sciences*

*1 Beichen West Road*

*Beijing 100101*

*China*

*E-mail: byhu@ioz.ac.cn*

*Prof. Wei Li*

*The State Key Laboratory of Reproductive Biology*

*Institute of Zoology*

*Chinese Academy of Sciences*

*1 Beichen West Road*

*Beijing 100101*

*China*

*E-mail: liwei@ioz.ac.cn*

Received for publication May 1, 2015

Accepted after revision October 7, 2015

Prepublished on Liebert Instant Online XXXX XX, XXXX